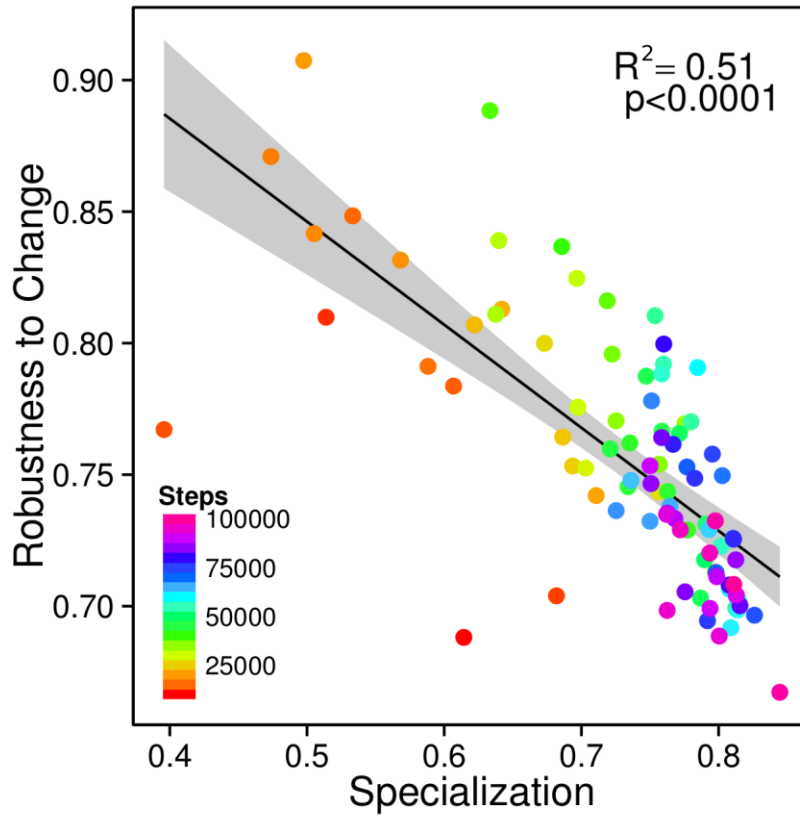
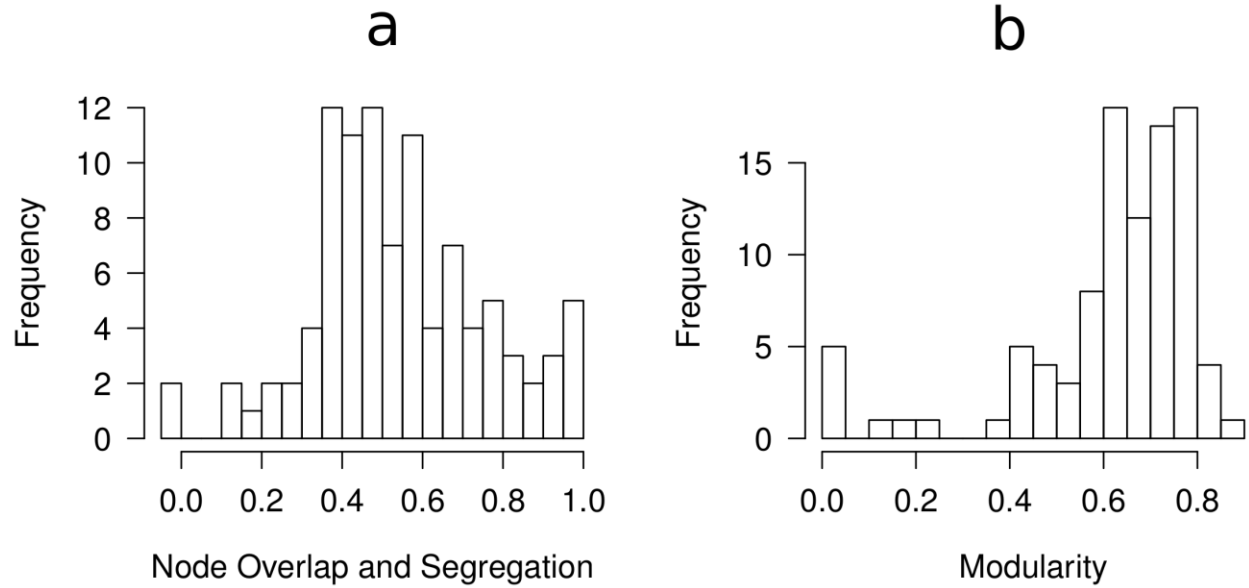


## Supplementary information

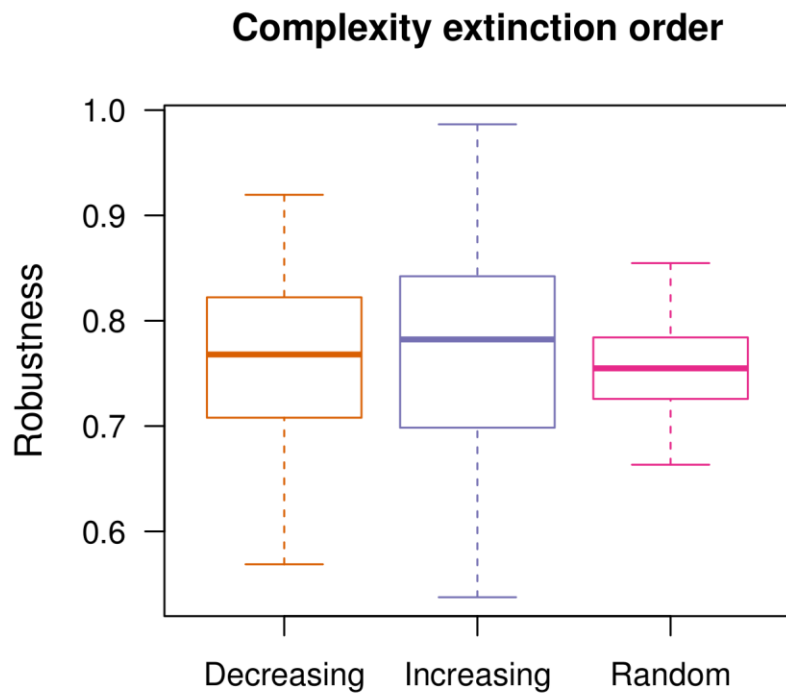
### Supplementary Figures



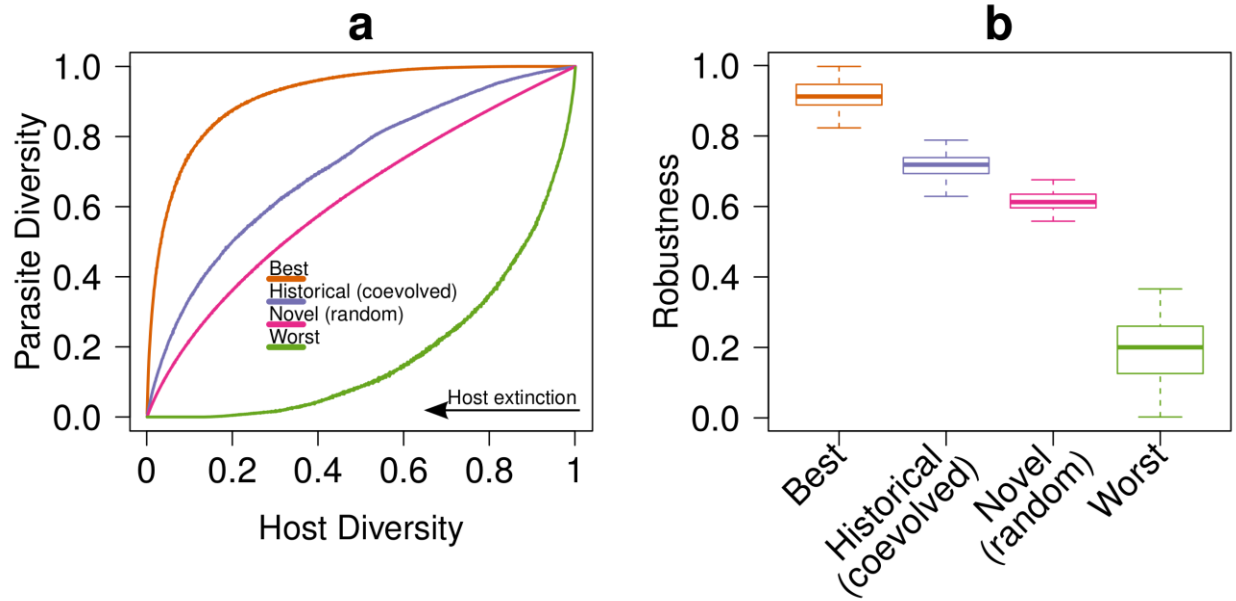
**Supplementary Figure 1 | Specialization in digital host-parasite assemblages increases over time, while robustness to novel conditions decreases.** Specialization was computed, in each digital host-parasite assemblage, as 1 minus the fraction of hosts used by all parasites.



**Supplementary Figure 2 | Distributions of node overlap and segregation (nestedness) values and modularity in the 100 co-evolved host-parasite networks. (a)** Most networks tends toward randomness (0) or nestedness (1), although no network tends toward segregation (< 0). **(b)** Most networks show high modularity.



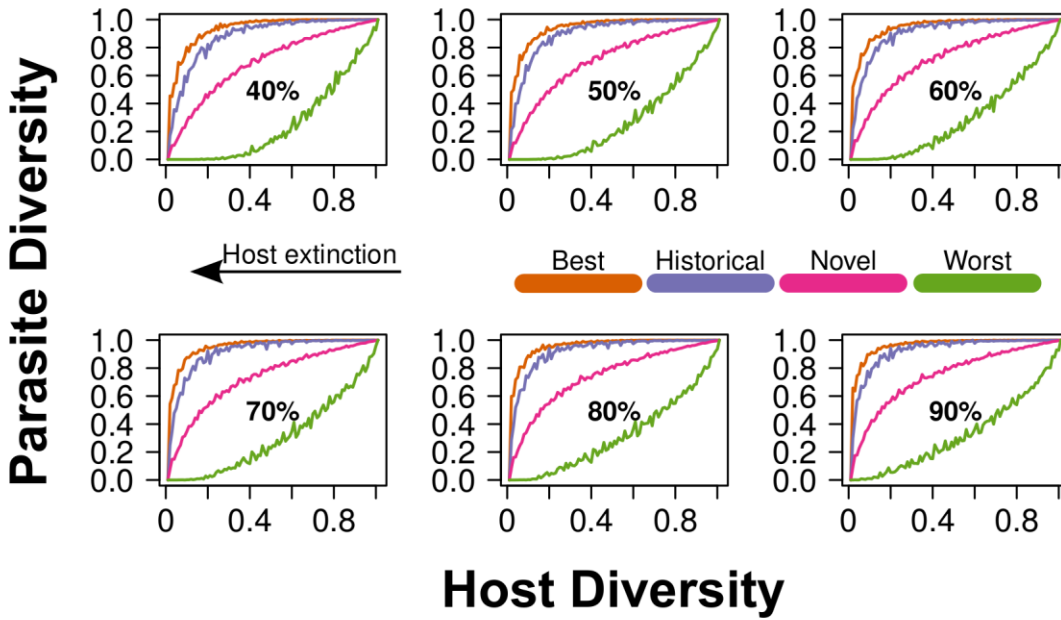
**Supplementary Figure 3 | Robustness of digital networks against the removal of hosts in decreasing, increasing and random order of complexity.** Host complexity was measured as the most complex of the host's tasks (see Methods). Boxes indicate first and third quartiles, whiskers indicate range values, and horizontal lines indicate median values.



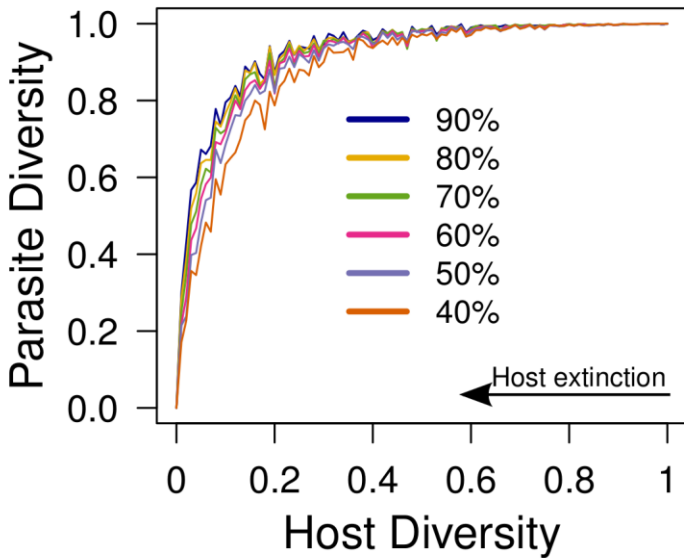
**Supplementary Figure 4 | Results of host-removal experiments in digital networks obtained by using organisms' genotypes as taxonomic units (instead of tasks). a)**

Average fraction of parasite species remaining in the digital host-parasite network after the subsequent removal of all host species according to historical conditions (from right to left) in all the experiments, contrasted with a best and a worst-case scenario, and a novel (random) scenario.

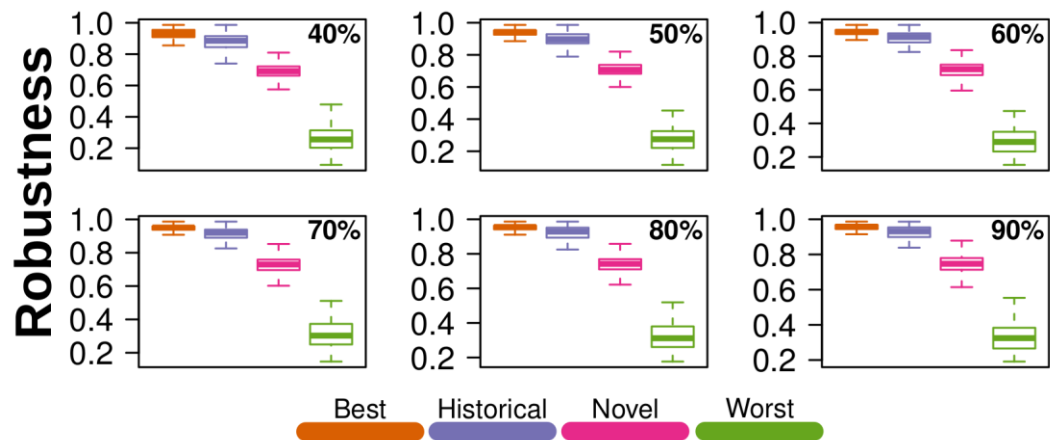
**b)** Robustness (the areas under curves in the four host removal scenarios) of the digital host-parasite networks under different scenarios of host removal. Boxes indicate first and third quartiles, whiskers indicate range values, and horizontal lines indicate median values.



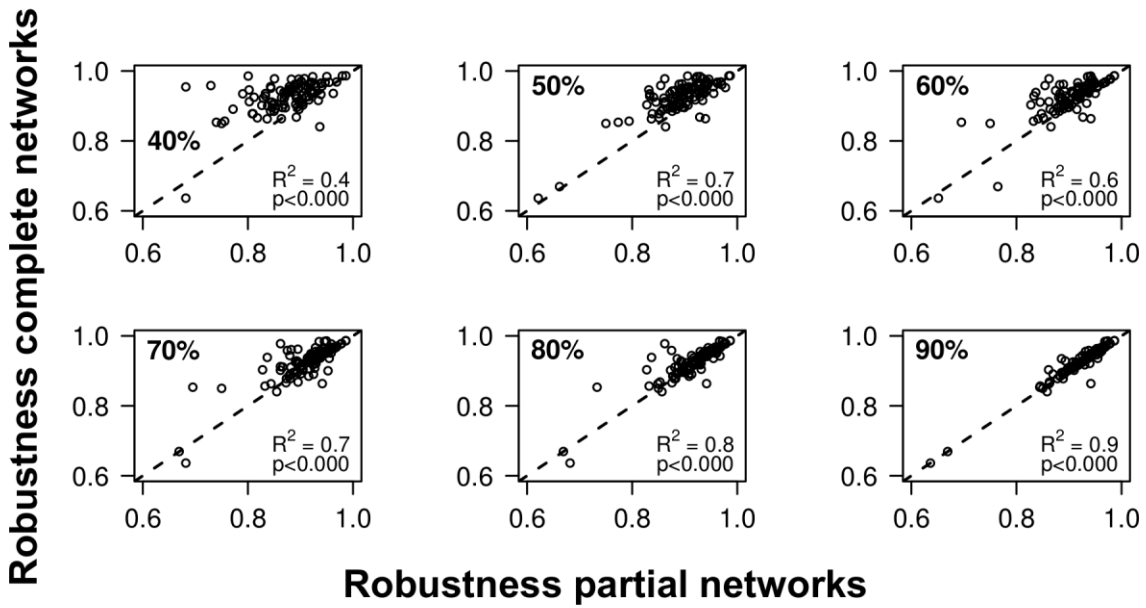
**Supplementary Figure 5 | Disassembling partial networks.** Average fraction of parasite species remaining in partial networks including random samples of 40%, 50%, 60%, 70%, 80% and 90% of the original edges after the subsequent removal of all host species according to the actual order of extinction observed in all experiments (historical), contrasted with a best-case and a worst-case scenario, and a novel (random) scenario.



**Supplementary Figure 6 | Comparison between historical disassembly in partial networks of increasing size.** Average fraction of parasite species remaining in partial networks including random samples of 40%, 50%, 60%, 70%, 80% and 90% of the original edges after the subsequent removal of all host species according to the actual order of extinction (i.e., historical) observed in all experiments.

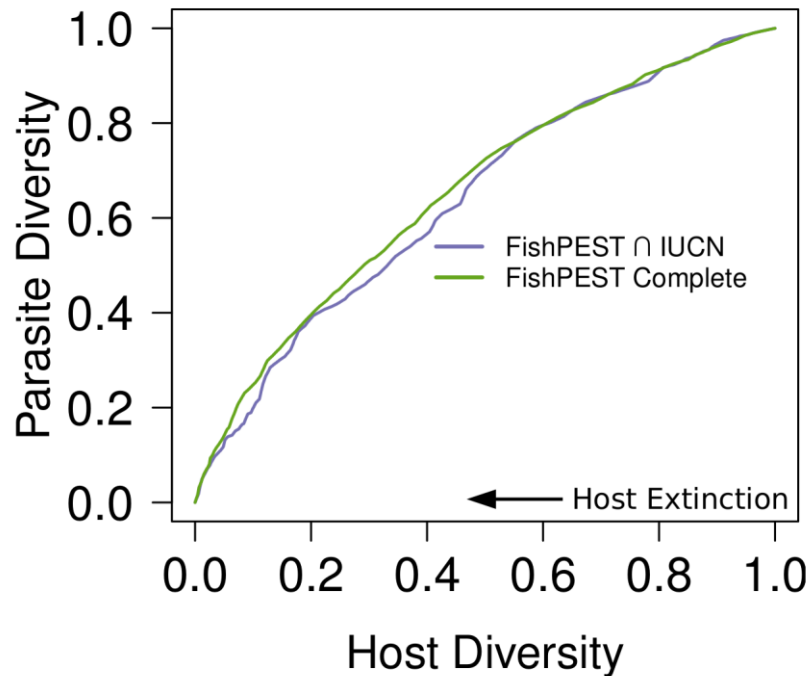


**Supplementary Figure 7 | Parasite assemblage robustness in partial networks.** Boxplots of the robustness obtained in partial networks including random samples of 50%, 60%, 70%, 80% and 90% of the original edges resulting from the subsequent removal of all host species according to the actual order of extinction observed in all experiments, contrasted with a best and a worst case scenario, and a novel (random) scenario. Boxes indicate first and third quartiles, whiskers indicate range values, and horizontal lines indicate median values.



**Supplementary Figure 8 | Comparison between parasite assemblage robustness in complete and partial networks.** Relationships between the robustness resulting from disassembling the complete digital host-parasite networks according to the observed extinction risks and the corresponding robustness values obtained from partial networks including random samples of 40%, 50%, 60%, 70%, 80% and 90% of the original edges.





**Supplementary Figure 9 | Effect of data availability on the estimation of global fish parasite assemblage robustness under historical conditions.** Comparison between the historical robustness of the network based on the entire FishPEST database<sup>13</sup> and that of the same network filtered by excluding all host species not listed in IUCN red list, both disassembled according to intrinsic vulnerability values<sup>15</sup>. Disassembly was replicated 100 times randomizing the order of ties, and the results were averaged.

## Supplementary Tables

**Supplementary Table 1:** Environmental parameters in the Avida simulations, and the resulting properties of communities and host-parasite networks at the end of the co-evolutionary phase.

*Net resource availability* is the overall balance between in-flowing and out-flowing resource units per simulation step. *Carrying capacity* is the maximum possible number of simultaneously alive individuals, that is equal to the number of cells (which, in turn, is given by  $World\ width \times World\ height$ ). *Node Overlap/Segregation* and *Modularity* were computed according to the procedure described in Strona and Veech<sup>36</sup>. *Host/parasite interactions* corresponds to the number of links in the host/parasite networks.

	Min.	1st Qu.	Median	Mean	3rd Qu.	Max.	St. Dev.
<i>Maturity (number of steps)</i>	101000	175500	259500	264200	334250	491000	104609
<i>Number of resources</i>	1.00	4.00	5.00	4.74	6.00	8.00	1.78
<i>Net resource availability</i>	21.4	54.5	66.9	72.2	81.2	166.0	28.8
<i>World width</i>	50.0	65.0	83.0	83.8	104.0	119.0	22.0
<i>World height</i>	50.0	67.8	84.0	84.3	103.3	119.0	20.6
<i>Carrying capacity</i>	2862	5118	6671	7007	8270	13216	2390
<i>Node Overlap/Segregation</i>	-0.04	0.40	0.53	0.54	0.68	1.00	0.22
<i>Modularity</i>	0.00	0.59	0.66	0.62	0.74	0.85	0.20
<i>Number of host phenotypes</i>	1.0	15.0	21.0	23.1	27.3	65.0	11.6
<i>Number of parasite phenotypes</i>	2.0	7.8	14.0	21.6	31.0	80.0	19.3
<i>Host/parasite interactions (phenotypes)</i>	3	42	88	133	179	670	128
<i>Number of host genotypes</i>	843	1534	2025	2211	2730	5463	934
<i>Number of parasite genotypes</i>	58	398	712	872	1126	3472	640
<i>Number of host individuals</i>	2575	3961	5388	5666	6924	13018	2201
<i>Number of parasite individuals</i>	140	1317	2566	2790	3626	8968	1891

**Supplementary Table 2:** Relationships (expressed as Spearman’s rank correlation coefficients) between the robustness of the digital host parasite networks obtained at the end of the co-evolutionary experiments, and the environmental features where the networks emerged (in terms of world dimensions and resource diversity/availability), network structural properties (node overlap/segregation, modularity, number of nodes, i.e. host and parasite phenotypes, and links, i.e. host/parasite interactions), genotypic and phenotypic diversity, and overall density of host and parasite individuals.

	<b>Robustness</b>			
	<i>Historical</i>	<i>Novel</i>	<i>Best</i>	<i>Worst</i>
<i>Maturity (steps)</i>	0.05	-0.06	0.04	0.05
<i>Resources</i>	-0.14	0.05	-0.12	0.02
<i>Net resource availability</i>	0.06	-0.08	-0.04	-0.05
<i>World width</i>	0.07	-0.05	0.20	-0.32
<i>World height</i>	-0.08	0.27	0.00	0.18
<i>Carrying capacity</i>	-0.07	0.14	0.08	-0.12
<i>Node Overlap/Segregation (raw value, <math>\hat{N}</math>)</i>	0.25	-0.13	0.26	-0.12
<i>Node Overlap/Segregation (effect size, <math>Z_N</math>)</i>	0.13	-0.18	0.10	-0.10
<i>Modularity</i>	-0.27	-0.05	-0.31	0.01
<i>Number of host phenotypes</i>	0.06	0.16	0.16	0.11
<i>Number of parasite phenotypes</i>	-0.05	0.18	0.03	0.01
<i>Host/parasite interactions (phenotypes)</i>	-0.01	0.31	0.08	0.15
<i>Number of host genotypes</i>	0.01	-0.06	0.08	-0.36
<i>Number of parasite genotypes</i>	0.03	0.13	0.03	0.14
<i>Number of host individuals</i>	-0.01	-0.02	0.08	-0.32
<i>Number of parasite individuals</i>	0.05	-0.04	0.00	0.14